online data

Hydrolysis of (1,4)-β-D-mannans in barley (*Hordeum vulgare* L.) is mediated by the concerted action of (1,4)-β-D-mannan endohydrolase and β-D-mannosidase

Maria HRMOVA*[1], Rachel A. BURTON*, Peter BIELY†, Jelle LAHNSTEIN* and Geoffrey B. FINCHER*[1]

*School of Agriculture, Food and Wine, University of Adelaide and Australian Centre for Plant Functional Genomics, Waite Campus, Glen Osmond, SA 5064, Australia, and †Institute of Chemistry, Slovak Academy of Sciences, Bratislava, Slovak Republic

A family GH5 (family 5 glycoside hydrolase) (1,4)-β-D-mannan endohydrolase or β-D-mannanase (EC 3.2.1.78), designated HvMAN1, has been purified 300-fold from extracts of 10-day-old barley (*Hordeum vulgare* L.) seedlings using ammonium sulfate fractional precipitation, followed by ion exchange, hydrophobic interaction and size-exclusion chromatography. The purified HvMAN1 is a relatively unstable enzyme with an apparent molecular mass of 43 kDa, a pI of 7.8 and a pH optimum of 4.75. The HvMAN1 releases Man (mannose or D-mannopyranose)-containing oligosaccharides of degree of polymerization 2–6 from mannans, galactomannans and glucomannans. With locust-bean galactomannan and mannopentaitol as substrates, the enzyme has K_m constants of 0.16 mg · ml^{-1} and 5.3 mM and k_{cat} constants of 12.9 and 3.9 s^{-1} respectively. Product analyses indicate that transglycosylation reactions occur during hydrolysis of (1,4)-β-D-manno-oligosaccharides. The complete sequence of 374 amino acid residues of the mature enzyme has been deduced from the nucleotide sequence of a near full-length cDNA, and has allowed a three-dimensional model of the HvMAN1 to be constructed. The barley *HvMAN1* gene is a member of a small (1,4)-β-D-mannan endohydrolase family of at least six genes, and is transcribed at low levels in a number of organs, including the developing endosperm, but also in the basal region of young roots and in leaf tips. A second barley enzyme that participates in mannan depolymerization through its ability to hydrolyse (1,4)-β-D-manno-oligosaccharides to Man is a family GH1 β-D-mannosidase, now designated HvβMANNOS1, but previously identified as a β-D-glucosidase [Hrmova, MacGregor, Biely, Stewart and Fincher (1998) J. Biol. Chem. **273**, 11134–11143], which hydrolyses 4NP (4-nitrophenyl) β-D-mannoside three times faster than 4NP β-D-glucoside, and has an action pattern typical of a (1,4)-β-D-mannan exohydrolase.

Key words: catalytic amine acid, (1,4)-β-D-mannan endohydrolase, β-D-mannosidase, family GH1 and GH5 glycoside hydrolases, *Hordeum vulgare*, transglycosylation.

INTRODUCTION

Man (mannose or D-mannopyranose)-containing polysaccharides are widely distributed in the cell walls of higher plants [1]. The chemical structures of these polysaccharides are based on a backbone of (1,4)-linked β-D-mannosyl residues, although other glycosyl residues are sometimes present in the main chain. Structurally, Man-containing polysaccharides fall into four main classes: (i) unsubstituted (1,4)-β-D-mannans, (ii) galactomannans, (iii) glucomannans and (iv) galactoglucomannans. Unsubstituted (1,4)-β-D-mannans are found in both leguminous and non-leguminous seeds, where they function as a carbohydrate reserve [1]. The homopolysaccharide (1,4)-β-D mannans have a crystalline structure, similar to cellulose. Galactomannans also function as energy reserves and are particularly abundant in the endosperm of seeds from the Leguminosae family. Galactomannans have a (1,4)-β-D-mannan main chain that is substituted at C(O)6 with single α-D-galactosyl residues. The degree of substitution depends on the plant species and the method used to extract the polysaccharide, but can range from less than 2% to essentially complete substitution [2,3]. The next major group of Man-containing polysaccharides comprises glucomannans that are linear copolymers of (1,4)-linked β-D-glucopyranosyl and β-D-mannopyranosyl residues with proportions varying from 1:1 to 1:2.3 [4], depending on the source. Glucomannans may be further esterified with acetyl groups at C(O)2 or C(O)3 of mannosyl residues [5]. The last group galactoglucomannans are glucomannans that are substituted with single α-D-galactosyl residues at C(O)6 of the mannosyl and glucosyl residues. Glucomannans and galactoglucomannans are minor components of unlignified primary walls of dicotyledons and monocotyledons, but are abundant in lignified secondary walls of coniferous gymnosperms and the endosperm walls of lilies [1].

In the commercially important cereals and grasses of the Poaceae, Man-containing polysaccharides are minor cell-wall components. In barley coleoptiles, these polysaccharides account for less than 0.5% of total wall polysaccharides [6]. Similarly, Man-containing polysaccharides are generally minor constituents of walls of aleurone and starchy endosperm of wheat and barley grains, where they account for 2–3% by weight of the walls [7,8]. In certain rice cultivars (*Oryza sativa* L., ssp. *indica*), the endosperm walls may contain up to 17% Man-containing

Abbreviations used: CM-Sepharose, carboxymethyl-Sepharose; 3D, three-dimensional; DP, degree of polymerization; EST, expressed sequence tag; GH1, family 1 glycoside hydrolase; HEC, hydroxyethylcellulose; IEF, isoelectric focusing; LB-GM, locust-bean gum galactomannan; Man, mannose or D-mannopyranose; Man2, mannobiose; Man3, mannotriose; Man5, mannopentaose; Man6, mannohexaose; 4NP, 4-nitrophenyl; 4NP-Glc, 4NP β-D-glucopyranoside; 4NP-Man, 4NP β-D-mannnopyranoside; OBR-LB-GM, Ostazin-Brilliant Red-dyed LB-GM; Q-PCR, quantitative real-time PCR; rmsd, root mean square deviation.

[1] Correspondence may be addressed to either of these authors (email maria.hrmova@adelaide.edu.au or geoff.fincher@adelaide.edu.au).

The nucleotide and amino acid sequence of the barley HvMAN1 mature enzyme reported in this paper was deposited in the DDBJ, EMBL, GenBank® and GSDB Nucleotide Sequence Databases with the accession number DQ356891.

polysaccharides [9], but in general terms, wall-associated mannans are unlikely to constitute a major source of metabolizable carbohydrate in cereal grains following germination, and are more likely to play a role in wall structure.

Interest in the mobilization of galactomannans from the walls of legume seeds during seed germination has led to numerous studies on (1,4)-β-D-mannan endohydrolases, α-D-galactosidases and β-D-mannosidases that mediate the complete enzymic depolymerization of the galactomannans to individual monosaccharide units [10–14]. In contrast, no information is available on these enzyme classes in germinating grains of cereals or grasses from the Poaceae. Although Man-containing polysaccharides are minor components of cell walls of coleoptiles, the starchy endosperm and aleurone of cereals, we now report (1,4)-β-D-mannan endohydrolases in extracts of young barley seedlings. One isoform of the barley enzyme has been purified and extensively characterized, its corresponding cDNA isolated, and a 3D (three-dimensional) model built and reconciled with mechanism of action of the enzyme. In addition, β-D-mannosidase, now designated HvβMANNOS1, capable of hydrolysing (1,4)-β-D-manno-oligosaccharides to Man has also been purified from the seedling extracts. Its amino acid sequence is identical with that of a family GH1 (family 1 glycoside hydrolase) β-D-glucosidase that has previously been characterized, and considered to be more correctly described as a polysaccharide exohydrolase [15,16]. Here, the enzyme is shown to have a marked preference for (1,4)-β-D-manno-oligosaccharides.

EXPERIMENTAL

Materials

DEAE-cellulose (DE52) was from Whatman (Maidstone, England), CM-Sepharose (carboxymethyl-Sepharose) CL-6B, Ampholine™ IEF (isoelectric focusing) polyacrylamide gels (pH range 3.5–9.5) and molecular-mass marker proteins (20–94 kDa) were from Amersham Biosciences (Uppsala, Sweden), Bio-Gel P-60, butyl-Sepharose and pI marker proteins were from Bio-Rad Laboratories (Richmond, CA, U.S.A.), Microcon microconcentrators were from Amicon (Beverly, MA, U.S.A.) and Kieselgel 60 thin-layer plates were from Merck (Darmstadt, Germany). Miracloth, 2-mercaptoethanol, PMSF, Dowex 50WX4-100 in the H^+ form, orcinol, BSA, 4NP (4-nitrophenyl) glycosides, HEC (hydroxyethyl cellulose) of medium viscosity, and laminarin (from *Laminaria digitata*) were from Sigma Chemical Co. (St. Louis, MO, U.S.A.). The Coomassie Protein Assay Reagent was from Pierce (Rockford, IL, U.S.A.), acetonitrile was from BDH Laboratory Supplies (Poole, U.K.) and barley (1,3,1,4)-β-D-glucan, ivory nut mannan, konjac glucomannan, 6^1-α-D-galactosyl Man3 (mannotriose), 6^3,6^4-di-α-D-galactosyl Man5 (mannopentaose) and (1,4)-β-D-manno-oligosaccharides of DP (degree of polymerization) 2–6 [Man2–Man6 (mannobiose to mannohexaose)] were from Megazyme (Bray, Ireland), CM-cellulose (carboxymethylcellulose) of degree of substitution 0.54 was from Imperial Chemical Industries (Dingley, Australia), and beechwood 4-*O*-methyl-(1,4)-β-D-glucuronoxylan was from Institute of Chemistry (Bratislava, Slovak Republic). The collection of native and modified galactomannans from guar was provided by Dr Francois Taravel (Centre de Recherches sur les Macromolécules Végétales, Centre National de la Recherche Scientifique, Grenoble, France), pustulan from *Umbilicaria pustulata* was provided by Professor Bruce Stone (La Trobe University, Melbourne, Australia) and tamarind xyloglucan was donated by Professor Vladimir Farkas (Institute of Chemistry, Bratislava, Slovak Republic). The α-D-mannans from *Candida utilis*, *Ca. albicans* and *Ca. krusei* were provided by Dr Josef Sandula (Institute of Chemistry, Bratislava, Slovak Republic). A low-viscosity LB-GM (locust-bean gum galactomannan) and OBR-LB-GM (Ostazin–Brilliant Red-dyed LB-GM) were prepared as described in [17].

Screening for β-D-mannan endohydrolases in barley extracts

Barley extracts prepared from ungerminated grain and grain germinated for 0–14 days (2-day increments) were adjusted to 90 % (w/v) saturation by addition of solid $(NH_4)_2SO_4$ [18]. The extracts were dialysed to equilibrium in 50 mM sodium acetate buffer (pH 5.0) containing 3 mM 2-mercaptoethanol. The β-D-mannan endohydrolase activities of barley extracts were measured by semi-quantitative radial diffusion assay [17] as follows. Rows of wells, 2–3 mm diameter, were punched out from a 2 mm thick agar medium, containing 100 mM sodium acetate buffer (pH 5.0), 0.1 % (w/v) OBR-LB-GM and 1.2 % (w/v) agar, in 80 mm diameter Petri dishes. Dialysed barley extracts (10–20 μl) were placed into the wells of the agar medium in the Petri dishes and the extracts were incubated for 3 h at 30 °C under 80–90 % (w/w) moisture content. The agar medium was de-stained with a mixture of ethanol/0.2 M sodium acetate buffer (pH 5.0) (2:1, v/v), and the widths of the cleared zones corresponding to the degraded zones of OBR-LB-GM were measured.

Enzyme extraction and purification of the β-D-mannan endohydrolase HvMAN1

Barley (*Hordeum vulgare* L., cv. Clipper) (3.5 kg dry weight) was surface sterilized for 10 min in 0.1 % (v/v) NaOCl, washed successively with sterile water, 0.5 M NaCl and sterile water, and steeped for 24 h in sterile water containing chloramphenicol (100 μg/ml), neomycin (100 μg/ml), penicillin G (100 units/ml) and nystatin (100 units/ml). Germinated grains were maintained at approx. 40 % (w/w) moisture content by regular application of fresh antibiotic solution for 10 days in the dark at 21 ± 2 °C. Bacterial or fungal contamination of the grains was not evident at any stage during this period. The germinated grain and young seedlings were homogenized at 4 °C in 1.5–2.0 vol. of 0.1 M sodium acetate buffer (pH 5.0) containing 10 mM EDTA, 10 mM sodium azide, 3 mM 2-mercaptoethanol and 3 mM PMSF, in a Waring blender for 5×60 s intervals with intermittent cooling (30 s) on ice. The homogenate was held for 1 h at 4 °C to extract proteins, insoluble material was removed by centrifugation (4000 ***g***, 30 min and 4 °C) and the extract was filtered through Miracloth. The extract was fractionally precipitated with $(NH_4)_2SO_4$ as described in [18].

Isolation and purity of the barley β-D-mannosidase HvβMANNOS1

The enzyme was purified from a homogenate of 10-day-old barley seedlings as described previously [19]. The purity of the enzyme was assessed by SDS/PAGE, where a single protein band was detected at high protein loadings, and by N-terminal amino acid sequence analysis [19].

Protein determination, SDS/PAGE and amino acid sequencing

Protein concentrations during purification and characterization, SDS/PAGE and amino acid sequence analyses were determined as described previously [18–20].

IEF

The crude protein extracts and purified preparations were separated on a flat-bed IEF apparatus (Amersham Biosciences) in 1 mm polyacrylamide gels using a pH gradient 3.5–9.5.

Pre-focused gels were run at 600 V for 30 min, followed by 800 V for a further 20 min. Proteins were detected with Coomassie Brilliant Blue after the gels were fixed in 20 % (w/v) trichloroacetic acid. Apparent pI values were estimated by reference to marker proteins with pI values 4.45–9.6. Enzyme activity in gels was detected by immediately overlaying the separation gels with a 1.5 mm-thick 1.5 % (w/v) agarose detection gel containing 0.5 % (w/v) OBR-LB-GM [17]; the contacted separation and detection gels were incubated for 1–2 h at 30 °C. The detection gels were immediately fixed and de-stained in 1.5–2.0 vol. of ethanol/0.2 M sodium acetate buffer (pH 5.0) (2:1, v/v). The areas of the detection gel with the hydrolysed OBR-LB-GM were de-stained in ethanol/0.2 M sodium acetate buffer (pH 5.0) (2:1, v/v) for several hours, depending on the activity of the preparation under investigation.

Enzyme assays

The activities of HvMAN1 and HvβMANNOS1 were determined at 30 °C in 100 mM sodium acetate buffers (pH 4.75 and 5.0) containing as substrates 0.2 % (w/v) LB-GM and 6.5 mM 4NP-Glc (4NP β-D-glucopyranoside) respectively; 0.02 % (w/v) BSA was present in all assays. The reactions with LB-GM were terminated by the addition of the alkaline copper reagent [21] and the rates of hydrolysis of polymeric substrates were determined from the increase in reducing sugars [21,22]. The hydrolytic rates on 4NP glycosides were determined spectrophotometrically at 410 nm [19]; the reactions were terminated by the addition of saturated sodium tetraborate solution (pH 9.0). One unit of activity is defined as the amount of enzyme that is required to release 1 μmol of Man from LB-GM per min. Specific activities are calculated per mg of protein, which was determined by the Coomassie Protein Assay Reagent as described previously [18]. One unit corresponds to 16.67 nanokatals.

Substrate specificities

Soluble and insoluble polysaccharides were used at final concentrations of 0.5 % (w/v), and 4NP glycosides were used in the concentration ranges of 4.3 mM (disaccharides) to 7.4 mM (monosaccharides). The incubation mixtures contained 100 mM sodium acetate buffer (pH 4.75) and 4–8 nM HvMAN1 and 0.02 % BSA, or 100 mM sodium acetate buffer (pH 5) and 8–10 nM HvβMANNOS1 and 0.02 % BSA; all incubations were at 30 °C. The rates of hydrolysis of polymeric substrates were determined from the increase in reducing sugars and the rates on 4NP glycosides from spectrophotometric measurements at 410 nm as described above.

Action patterns

Monosaccharide and oligosaccharide products released during initial stages of enzymic hydrolyses by HvMAN1, with and without addition of HvβMANNOS1, were assayed in incubation mixtures containing 10 mM sodium acetate buffer (pH 4.75) and 0.5 % LB-GM, or 1 mM Man4 (mannotetraose)–Man6. The reaction mixtures contained 4 nM HvMAN1, and when required 8 nM HvβMANNOS1. The hydrolysis of LB-GM was followed for 1 and 4 h and the reaction mixtures with Man4–Man6 were incubated for 7 and 14 min at 30 °C. The final hydrolysis products released from LB-GM were examined in the same way as described above, except that after 4 h the initial amounts of the fresh enzyme(s) were added and the reactions were allowed to proceed for a total of 18 h. The reactions were stopped by heating to 100 °C for 1 min and hydrolysis products were analysed by TLC on silica-gel plates or by HPLC. The hydrolytic rates on Man4–Man6 were quantified by HPLC. The capacity of HvMAN1 to catalyse transglycosylation reactions was evaluated by incubating 4 nM HvMAN1 at 30 °C for 2, 20 and 60 min in 10 mM sodium acetate buffer (pH 4.75) with 10 mM Man4. Hydrolysates were applied to silica-gel plates (layer thickness 0.2 mm), developed in ethyl acetate/acetic acid/water (3:2:1, by vol.) and reducing sugars were detected using the orcinol reagent [18].

Rates of hydrolysis of Man2–Man6 by the HvβMANNOS1 were measured at final substrate concentrations of 1 mM in 100 mM sodium acetate buffer (pH 5.0) containing 0.02 % BSA for 4 and 8 min at 30 °C. The incubation mixtures contained 16 nM HvβMANNOS1. Products released from the individual oligosaccharides were quantified by HPLC and the extent of hydrolysis was calculated from the integrated areas of the substrate and product peaks. Standards Man and oligosaccharides Man2–Man6 were used for calibration.

Kinetic analyses

The kinetic parameters K_m and k_{cat} were determined by measuring initial hydrolysis rates of 2–4 nM HvMAN1 with LB-GM and mannopentaitol in concentration ranges that were 0.3–3 times the calculated K_m constants. Man5 was reduced to its alditol form by a standard procedure using sodium borohydride [23]. Assays were performed in triplicate in 100 mM sodium acetate buffer (pH 4.75) containing 0.02 % BSA. Enzymic reactions were terminated by the Somogyi alkaline copper reagent and the hydrolytic rates were determined from the increase in reducing sugars as described above. Standard errors for mannoheptaitol and LB-GM were within 4–10 %. The kinetic constants were calculated using a non-linear regression analysis [24] and the GraFit program [25].

pH optimum, thermal and freeze/thaw stabilities

The effect of pH on the rate of hydrolysis of 0.2 % LB-GM was determined by incubating 2 nM HvMAN1 at 30 °C for 40 min in 50 mM citric acid/100 mM sodium dihydrogen phosphate (McIlvaine) buffers (pH 3–7) in the presence of 0.02 % BSA. The estimates of apparent pK_a values, based on a single pK_a model equation [25], were determined from non-linear fitting of the line through the individual data points of the pH dependence curve. Thermal stabilities of HvMAN1 were determined after 15 min incubation at 0–70 °C (10 °C increments) and 0.5 % LB-GM, with and without 0.02 % BSA. Freeze/thaw stabilities of HvMAN1 at 2 nM concentrations were determined after five freeze (−80 °C)/thaw (4 °C) cycles (each step had a duration of 2 min) at 30 °C in 100 mM sodium acetate buffer (pH 4.75) and 0.5 % LB-GM, with and without addition of 0.02 % BSA.

Co-operativity of barley HvMAN1 and HvβMANNOS1

The hydrolysis of dialysed (exclusion limit 10 kDa) 0.5 % (w/v) LB-GM was monitored in 100 mM sodium acetate buffer (pH 4.75) containing 0.02 % (w/v) BSA, 4 nM HvMAN1 and 4, 8 and 16 nM HvβMANNOS1 at 30 °C. The reaction progress was followed by the increase in reducing sugars as described above. The hydrolysis of 1 mM Man2 to Man6 was followed by incubating 4 nM HvMAN1 and 8 nM HvβMANNOS1 in 10 mM sodium acetate buffer (pH 4.75) for 15 min at 30 °C, and the hydrolysis products were quantified by HPLC.

HPLC analyses of enzymic hydrolysates

Samples of hydrolysates and standards were freeze-dried, redissolved in 15 μl of MilliQ water (conductivity 18 μS) and diluted with an equal volume of acetonitrile; injection volumes were 25 μl. A model 1090 liquid chromatograph with autosampler and diode-array detector, controlled by ChemStation software

(Agilent Technologies, Palo Alto, CA, U.S.A.) was used for HPLC. The chromatography was performed on a Prevail Carbohydrate ES column (250 mm × 4.6 mm, 5 μm particle size) (Alltech Associates, Deerfield, IL, U.S.A.). The column temperature during the chromatographic runs was 21 °C and the flow rate was 0.6 ml/min. A linear gradient of 30 to 100 % eluent (B) was used for elution, where eluent (A) is 90 % (v/v) acetonitrile and (B) is 40 % (v/v) acetonitrile. The sugars were detected by absorbance at 192 nm. Integration of peak areas, calibration, and calculation of oligosaccharide amounts were carried out using ChemStation software (Agilent Technologies).

RNA isolation

Total RNA was isolated from the whole seedlings (*H. vulgare* L., cv. Clipper) 9 days after germination and from other plant tissues using the TRIzol® reagent (Invitrogen, Carlsbad, CA, U.S.A.) [26]. First strand cDNA was prepared from 3 μg of total RNA using an oligo$(dT)_{20}$ primer and Superscript III reverse transcriptase (Invitrogen) as recommended by the manufacturer. A cDNA fragment of 560 bp was amplified from the seedling cDNA population by PCR, using a programme of 35 cycles of denaturation (94 °C, 30 s), annealing (50 °C, 30 s) and extension (72 °C, 1 min). The reaction contained Taq DNA polymerase (Invitrogen), Taq DNA Polymerase PCR buffer (200 mM Tris/HCl, pH 8.4, containing 500 mM KCl and supplied with 1 ml of 50 mM $MgCl_2$) as specified by Invitrogen, 5 mM dNTPs, 10 % (v/v) dimethyl sulfoxide and 10 μM of degenerate oligonucleotide primers designed for tryptic fragments 2 and 4 of HvMAN1 (Figure 6) of the sequences 5′-GAYGAYGAYTTYTTYACNGA-3′ (tryptic fragment 2) and 5′-ACNATGCARGCNTGGGTNGC-3′ (tryptic fragment 4). The PCR product was purified with a QIAquick column (Qiagen, Valencia, CA, U.S.A.). The sequence of the PCR product was confirmed using BigDye3 chemistry on an ABI 3700 capillary sequencer (Applied Biosystems, Foster City, CA, U.S.A.) and was found to contain the amino acid sequence of tryptic fragment 3 (Figure 6).

DNA isolation and genomic walking

Genomic DNA was isolated from young barley (*H. vulgare* L., cv. Clipper) leaf tissue [27]. Aliquots of the purified DNA were digested with a range of blunt-ended restriction enzymes, which were used for a genomic walking procedure [26] in both the upstream and the downstream directions, using the 560 bp PCR fragment described above as a starting point for primer design. The fragments generated by this procedure were purified from the PCR reaction mixture, sequenced and analysed for the presence of introns, and for the presence of coding region sequences similar to other plant β-D-mannan endohydrolase sequences and to tryptic fragments 1 and 5 of HvMAN1 (Figure 6). Finally, a cDNA fragment corresponding to the complete amino acid sequence of the mature enzyme was isolated and completely sequenced in both directions.

Transcript analysis

Levels of barley HvMAN1 mRNAs were determined by Q-PCR (quantitative real-time PCR) in an RG 2000 Rotor-Gene Real Time thermal cycler (Corbett Research, Sydney, Australia) as described in [26]. Primer pairs for five control genes, namely *α-tubulin*, *cyclophilin*, *GAPDH*, HSP70 and *HvCesA1*, are listed in [26]. Forward and reverse primers for the *HvMAN1* gene were as follows: 5′-GGACGACTACTGCGCATGGTG-3′ and 5′-GACGGAACGCACACCCAAGCTAGC-3′.

PCR products for making stock solutions were obtained from barley coleoptile leaf cDNA (1 μl) in a reaction mixture containing 10 μl of QuantiTect SYBR® Green PCR reagent (Qiagen), 3 μl each of 4 μM forward and reverse primers and 3 μl of water under the following cycling parameters: pre-step 15 min at 95 °C; 45 cycles of 20 s at 95 °C, 30 s at 55 °C, 30 s at 72 °C; and an extension step 15 s at 80 °C. The amplification products pooled from four to six independent 20 μl PCR reactions were purified and quantified by HPLC on a Varian HELIX DNA column (2.1 mm × 15 cm, 3.5 μm; Varian, Middelburg, The Netherlands). Chromatography and product quantification were performed as described in [26]. The PCR product was used to make a dilution series covering seven orders of magnitude (10^7 to 10^1 copies/μl).

The optimal temperature for data acquisition for each pair of primers was determined from melting-curve analysis after heating PCR products, at the end of the amplification, from 70 to 99 °C and monitoring fluorescence intensity. For measuring transcript levels in tissue samples, 1 μl of a 1:10 dilution of a cDNA population was used to prepare a similar PCR reaction mixture as described above, but with addition of 0.6 μl of 10× SYBR® Green and 2.4 μl of water. Quantitative PCR was performed with cycling parameters similar to those described above, but with a modified extension step at the optimal acquisition temperature for 15 s. The Rotor-Gene v4.6 software (Corbett Research) was used for data acquisition and manipulation. For comparisons of mRNA levels in different tissues, normalization factors were calculated from at least three control genes [26].

Phylogenetic analysis

The amino acid sequences of barley HvMAN1 (*H. vulgare* L., cv. Clipper) (the present study), lettuce (*Lactuca sativa* L.) (Swiss-Prot accession number Q93X40), tomato (*Lycopersicum esculentum* Mill, cv. Castalia) (Q8L5J1) and rice (*O. sativa*, subsp. *japonica*) (Q8LR27) and ten other plant amino acid sequences (Swiss-Prot accession numbers of the *Arabidopsis* entries Q9LW44, Q9SG95, Q9SG94, Q9FJZ3, Q9LZV3, Q9M0H6, Q9SKU9, tomato entries O48540, Q93WT4, Q8RVL3) were aligned with T-COFFEE server [28] and a phylogenetic tree for the 14 plant sequences was constructed (Figure 7).

Molecular modelling of HvMAN1

The 3D structural template of tomato β-D-mannan endohydrolase (Protein Data Bank accession number 1RH9) (http://www.rcsb.org/pdb/), called hereafter 1RH9, was provided by Dr Aaron J. Oakley (Research School of Chemistry, Australian National University, Canberra, Australia). The HvMAN1 and tomato β-D-mannan endohydrolases were aligned as described previously [29]. The WebANGIS Wisconsin genetics Computer Group suite of programs (http://www.angis.org.au/new/index.html) was used for calculation of sequence compatibilities between the target and the template protein sequences. To identify the topology of secondary structural elements and of the active sites, six other representatives of family GH5 (family 5 glycoside hydrolase) were chosen by automated BLAST search [30]. These amino acid sequences were structurally aligned with HvMAN1 and 1RH9 using the T-COFFEE server [28] and the 3D-PSSM fold recognition server (http://www.sbg.bio.ic.ac.uk/∼3dpssm/). Each individual entry was checked manually using hydrophobic cluster analysis [31] and PsiPred server (http://bioinf.cs.ucl.ac.uk/psipred/) to maintain the integrity of hydrophobic cluster patterns and the distribution of secondary-structure elements in the sequences. The structurally aligned HvMAN1 and 1RH9 sequences were subsequently used as input parameters to build a 3D model of the barley enzyme HvMAN1 with Modeller 7v7, which implements comparative modelling by satisfaction of empirical spatial

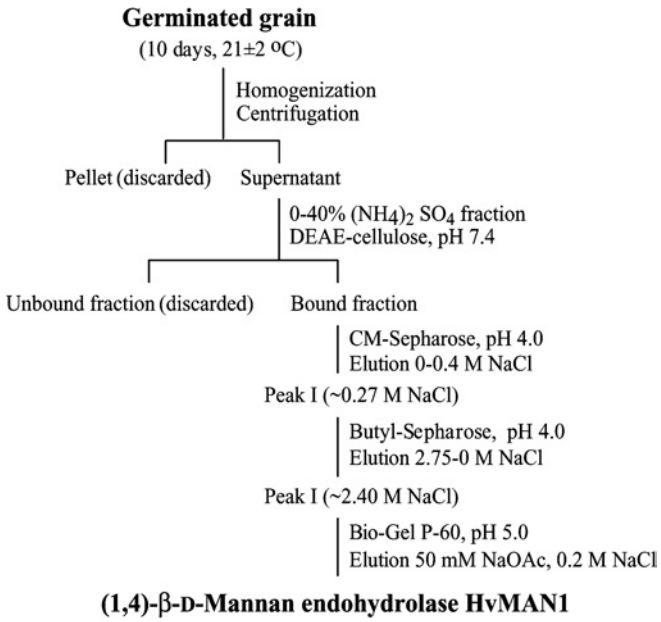

Scheme 1 Purification scheme of the barley β-D-mannan endohydrolase HvMAN1

restraints and statistical analysis of the relationships between pairs of structures with a common evolutionary origin [32]. The 3D molecular model of HvMAN1 was selected from 19 models; this model with the lowest value of the Modeller objective function was chosen for further refinement. The energy configuration output of the best model was used as a starting parameter for loop optimizations with a scan loop followed by energy minimization [29]. The stereochemical quality and overall G-factors of the final HvMAN1 model were calculated with PROCHECK [33]. The compatibility of the sequence with the overall fold was estimated using ProsaIIv3 [29]. The program 'O' [34] was used to determine the rmsd (root mean square deviation) values in the Cα backbone positions between the two 3D structures. The electrostatic potentials of the two enzymes were calculated with Poisson–Boltzmann equation using GRASPv1.3.6 [35], and mapped on to the molecular surfaces that were generated with a probe radius of 1.4 Å (1 Å = 0.1 nm). The molecular graphics were generated with the PyMol (http://www.pymol.org) and GRASP [35] packages.

RESULTS

Purification of the barley (1,4)-β-D-mannan endohydrolase HvMAN1

Prior to the development of the purification procedure, barley grain and young seedling extracts were tested semi-quantitatively for (1,4)-β-D-mannan endohydrolase activity using an agar diffusion plate assay with the dyed substrate OBR-LB-GM. Based on the diameters of the cleared zones on the plate, maximal activity was detected at approx. 10 days after germination (results not shown). Before 8 days and after 12 days, activity measured by this assay was essentially zero. Accordingly, the starting material for the large-scale purification of the enzyme was an extract of 10-day-old barley seedlings. In other preliminary experiments, it was shown that the β-D-mannan endohydrolase activity was highest in the 0–40 %-saturated $(NH_4)_2SO_4$ fraction (results not shown). IEF of this fraction showed one dominant form of the β-D-mannan endohydrolase, with a pI value of approx. 7.8 (results not shown). A minor form, with a pI value of 7.4, was detected in the 60–80 % $(NH_4)_2SO_4$ fraction, but this was not further purified. It remains to be established if the second isoform represents a post-translational modification of the major β-D-mannan endohydrolase with the pI value of 7.8 or whether it represents a second isoenzyme of β-D-mannan endohydrolase.

The final scheme used for the purification of the barley HvMAN1 enzymes is summarized in Scheme 1 and the corresponding yields and purification factors are shown in Table 1. A key purification step was CM-Sepharose, where the HvMAN1 was separated from major remaining protein peaks and from contaminating β-D-mannan endohydrolase activity (Figure 1). Hydrophobic interaction chromatography on butyl-Sepharose and size-exclusion chromatography on Bio-Gel P-60 were subsequently required to finally purify the enzyme to a near monodisperse form (Scheme 1; Table 1; Figure 2). When the protein profiles were examined at the various stages of purification, it was clear that the butyl-Sepharose step was also important for the removal of contaminating proteins (results not shown). The final purified enzyme preparation (lane 5 of Figure 2A) shows a single band of approx. 43 kDa, and no contaminating proteins are evident at high protein loadings. Furthermore, a single protein and activity band of pI 7.8 was detected on the IEF gel (Figure 2B, lane 1), and on a dyed locust-bean galactomannan (OBR-LB-GM) zymogram (Figure 2B, lane 2). A single sequence was also detected during N-terminal amino acid sequence analysis of the purified enzyme, where 95 % yields of the phenylthiohydantoin amino acid derivatives, normalized per mol of the total protein, were obtained. Finally, sequencing of tryptic peptides prepared from the purified (1,4)-β-D-mannan endohydrolase yielded single

Table 1 Enzyme yields and purification factors of HvMAN1 from 10-day-old barley seedlings

Purification stage	Yield		Specific activity (units/mg)	Recovery† (%)	Purification factor‡ (-fold)
	Protein (mg)	Activity* (unit)			
Crude homogenate	11545	1132	0.1	100	1
0–40 % $(NH_4)_2SO_4$	4756	646	0.14	57.1	1.4
DEAE-cellulose (pH 7.4)	81	113	1.4	10.0	14
CM-Sepharose (pH 4.0)	19	36	1.9	3.2	19
Butyl-Sepharose, 2.75 M NaCl	0.6	5.5	9.2	0.5	92
Bio-Gel P-60 (pH 5.0)	0.1	3.0	30	0.3	300

* Enzyme activities were assayed with LB-GM.
† Recoveries are expressed as percentage of crude-homogenate activity units.
‡ Purification factors are based on specific activities.

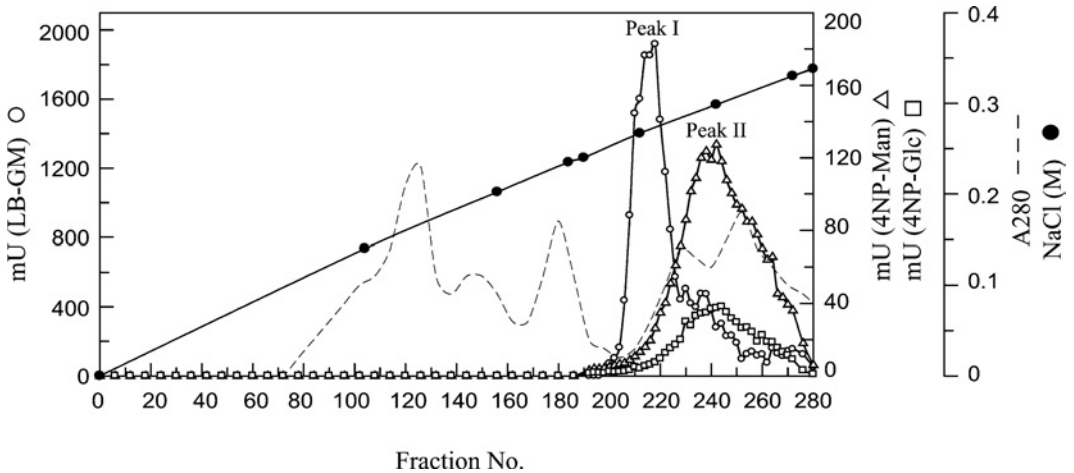

Figure 1 Ion-exchange chromatography of a barley seedling extract on CM-Sepharose during purification of HvMAN1

Material precipitated at 0–40 % saturated $(NH_4)_2SO_4$ was applied to DEAE-cellulose at pH 7.4 and unbound proteins were eluted. The material was then applied to a CM-Sepharose column at pH 4.0, and after unbound proteins washed through, bound proteins (– – –) were eluted with a linear gradient of 0–0.4 M NaCl (●). Fractions were assayed against LB-GM (○), 4NP-Man (△) and 4NP-Glc (□).

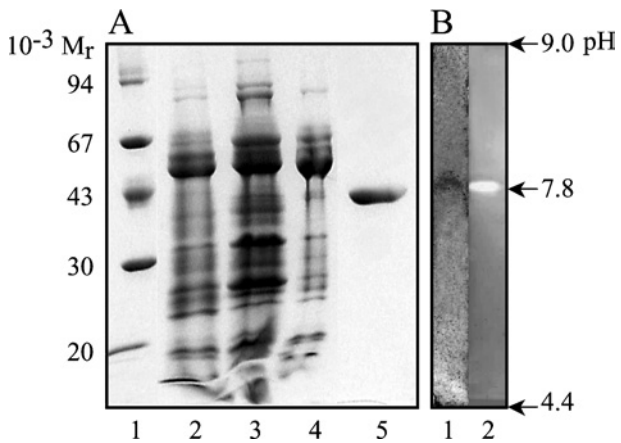

Figure 2 SDS/PAGE of protein fractions during purification of HvMAN1

(**A**) Lane 1, molecular-mass markers; lane 2, seedling homogenate; lane 3, 0–40 % $(NH_4)_2SO_4$ fraction; lane 4, CM-Sepharose pooled fractions 200–225; lane 5, purified HvMAN1 after Bio-Gel P-60. (**B**) Lane 1, purified HvMAN1 after Bio-Gel P-60; lane 2, activity zymogram of HvMAN1 with OBR-LB-GM. Proteins were detected with Coomassie Brilliant Blue. Average molecular masses are given in kDa (**A**), and pH boundaries of the gel and a pI point of HvMAN1 (**B**) are indicated.

peptide sequences with the expected phenylthiohydantoin amino acid derivative yields. Based on these results, we have concluded that the enzyme was purified to a near monodisperse form.

The purification procedure yielded approx. 100 μg of HvMAN1 enzyme from the initial extract from 3 kg dry weight of germinated barley grain. The final purification factor was 300, which is not as high as those achieved for other polysaccharide hydrolases from germinated barley [16,18,19]. The barley HvMAN1 proved to be a relatively unstable enzyme, particularly after freezing, and steadily lost activity during the purification process. The addition of 0.2 % BSA stabilized the purified enzyme both at elevated temperatures (see Supplementary Figure 1A at http://www.BiochemJ.org/bj/399/bj3990077add.htm) and after a number of freeze–thaw cycles (see Supplementary Figure 1B). A single freeze–thaw cycle in the absence of BSA resulted in the loss of more than 80 % of activity, but BSA stabilized the enzyme to the extent that it retained most of its activity after multiple freeze–thaw cycles (Supplementary Figure 1B). It is important to note that although the stability of the purified enzyme was assayed at a relatively low protein concentration, the barley HvMAN1 was purified to a near monodisperse form, and therefore, its instability could not be linked with a proteolytic degradation or to the presence of other enzyme species that could interfere with the activity measurements. Thus it is concluded that relatively low purification factor and recovery of purified enzyme, corresponding to approx. 0.3 % of initial activity (Table 1), were largely attributable to the inherent instability of the enzyme.

Table 2 Kinetic parameters of HvMAN1

Standard errors of triplicate assays were within 4–10 %.

Substrate	K_m	k_{cat}	k_{cat}/K_m
LB-GM	0.2 ± 0.02 mg/ml	12.9 ± 1.2 s^{-1}	80.9 ± 6.9 $s^{-1} \cdot ml \cdot mg^{-1}$
Mannopentaitol	5.3 ± 0.2 mM	3.9 ± 0.2 s^{-1}	0.7 ± 0.04 $s^{-1} \cdot mM^{-1}$

Enzymic properties of HvMAN1

The pH optimum of the purified enzyme was pH 4.75 (Supplementary Figure 2 at http://www.BiochemJ.org/bj/399/bj3990077add.htm). The kinetic properties of the purified HvMAN1 enzyme on LB-GM and mannopentaitol are compared in Table 2. The K_m values were 0.16 mg/ml and 5.3 mM respectively and the catalytic efficiencies (k_{cat}/K_m) were 80.9 $s^{-1} \cdot ml \cdot mg^{-1}$ and 0.7 $s^{-1} \cdot mM^{-1}$ respectively.

Substrate specificity of HvMAN1

The relative hydrolytic rates of the purified HvMAN1 enzyme from barley were compared on a range of unsubstituted and substituted (1,4)-β-D-mannans (Table 3). The results showed that highly substituted galactomannans and the substituted oligosaccharide 6^3,6^4-di-α-D-galactosyl Man5 were not hydrolysed. Galactomannans with a degree of galactosyl substitution of approx. 33 % were hydrolysed at the highest rate, but this rate decreased as the degree of substitution decreased or increased.

Table 3 Substrate specificity of HvMAN1

Substrate*	Source	Common name	Status	Man/Gal (Glc) ratio	Relative rate†
Mannan	*Phytelephas macroarpa* Ruiz & Pav	Ivory nut	Native	1.0:0	23.2
Galactomannan	*Cyamopsis tetragonoloba* (L.) Taub	Guar	Native	1.6:1	0
	Cy. tetragonoloba (L.) Taub	Guar	Modified	3.0:1	100
	Ceratonia siliqua L.	Locust-bean or garob	Native	3.5:1	71.2
	Cy. tetragonoloba (L.) Taub	Guar	Modified	6.3:1	65.3
Glucomannan	*Amorphophaiius konjac* (K. Koch.)	Konnyaku		4:3	70.2

* No hydrolytic activity was detected against *Ca. utilis*, *Ca. albicans* and *Ca. krusei* α-D-mannans, CM-cellulose, HEC, laminarin, pustulan, 1,3;1,4-β-D-glucan, 4-*O*-methyl-β-D-xylan, xyloglucan, 6^1-α-D-galactosyl mannotriose, 6^3,6^4-di-α-D-galactosyl mannopentaose, 4N glucoside, mannoside, galactoside, xyloside (α and β anomers), 4N gentiobioside and *N*-acetyl-β-D-glucosaminide.
† Hydrolysis rates are expressed as a percentage of the rate of HvMAN1 against guar galactomannan.

Table 4 Substrate specificity of HvMANNOS1

Substrate	Relative rate* (%)
4NP-Glc	34.5
4NP-Man	100
4NP-β-D-galactoside	4.6
4NP-*N*-acetyl-β-D-glucosaminide	0.7
4NP-β-D-xyloside	0.3
4NP-α-L-arabinofuranoside	0.5
4NP-gentiobioside	0
4NP-cellobioside	1.9

* Hydrolysis rates are expressed as a percentage of the rate against 4NP-Man.

The almost unsubstituted ivory nut mannan was hydrolysed more slowly than guar galactomannan with 33 % substitution (Table 3). An unsubstituted glucomannan was also hydrolysed relatively rapidly (Table 3). The enzyme had no activity on a range of α-D-mannans, β-D-glucans, β-D-xylans and other glycosides.

Purification of the barley HvβMANNOS1

As shown in Figure 1, relatively high levels of activity against 4NP-Man (4NP β-D-mannnopyranoside) were detected in extracts of young barley seedlings, and the putative β-D-mannosidase co-purified with β-D-glucosidase activity. It was suspected that a single enzyme might have been responsible for both the β-D-mannosidase and β-D-glucosidase activities, and the enzyme with the β-D-mannosidase activity was subsequently purified using procedures developed for the barley β-D-glucosidase isoenzyme βII (results not shown) [16]. Most importantly, the sequence of the first 80 amino acid residues of HvβMANNOS1 matched perfectly with barley β-D-glucosidase [15,16]. Re-examination of the substrate specificity of this enzyme showed that it had a marked preference for 4NP-Man (Table 4). When LB-GM was incubated for 30 min at 30 °C with HvMAN1 in the presence of HvβMANNOS1, an increase in the rate of LB-GM hydrolysis was clearly detectable (see Supplementary Figure 3 at http://www.BiochemJ.org/bj/399/bj3990077add.htm).

Action pattern of HvMAN1

The hydrolysis products released from LB-GM by the purified HvMAN1 enzyme included large amounts of Man3 and Man2 (Figure 3, left panel). Relatively little free Man accumulated, even after 18 h incubation at 30 °C. An abundant oligosaccharide product with mobility between those of Man4 and Man5 was observed and is believed to be a galactomanno-oligosaccharide of DP 4, carrying a single galactosyl residue. The mobility of this

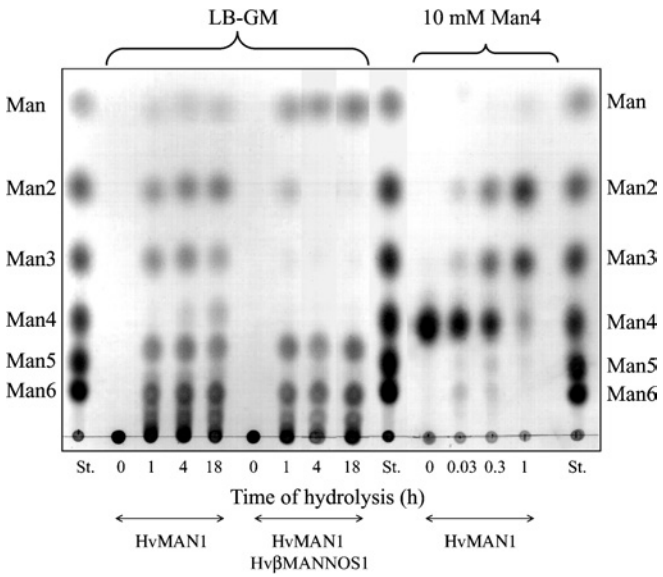

Figure 3 Mode of action of HvMAN1 on LB-GM without and with addition of HvβMANNOS1, and transglycosylation reaction of Man4 catalysed by HvMAN1

TLC of hydrolysis products released by HvMAN1 from LB-GM after 1, 4 and 18 h at 30 °C, without (lanes 2–5) and with (lanes 6–9) the addition of HvβMANNOS1. Lanes 11–14 show products released from 10 mM Man4 after 2, 20 and 60 min incubation at 30 °C. The presence of enzymes is also indicated by horizontal arrows. Standards (St.) are Man and (1,4)-β-D-manno-oligosaccharides Man2–Man6 (lanes 1, 10 and 15).

oligosaccharide during TLC was identical with that of standard 1^3-α-D-galactosyl Man3 (results not shown), but its detailed structure was not determined.

The major products released, when Man4 at 10 mM was incubated for 60 min at 30 °C with the HvMAN1 enzyme, were Man2 and Man3. However, the release of an equivalent amount of free Man was not observed. This observation together with the production of oligosaccharides larger than Man4 strongly suggested that the barley HvMAN1 is capable of catalysing transglycosylation reactions (Figure 3, right panel). Similar results were obtained when Man4 and longer manno-oligosaccharides, Man5 and Man6 (all at 1 mM), were incubated for 7 min at 30 °C with HvMAN1 (Figure 4). It was also clear from this analysis that the hydrolytic rates of manno-oligosaccharides Man4–Man6 increased with their DPs (Figure 4).

When the LB-GM was incubated for 1, 4 and 18 h at 30 °C with purified HvMAN1 in the presence of purified HvβMANNOS1, free Man was the major product, as expected (Figure 3).

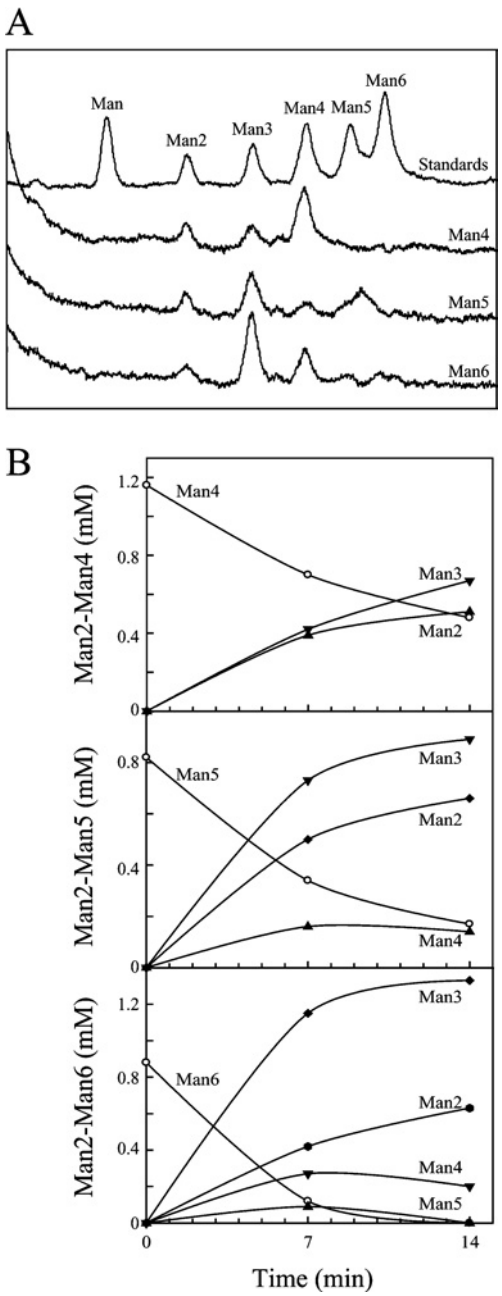

Figure 4 Time course of Man4–Man6 hydrolysis by HvMAN1

(**A**) HPLC analysis of hydrolysis products released from Man4–Man6 by HvMAN1. Hydrolysis products of Man4–Man6 are shown after 7 min incubation at 30 °C, when initial hydrolysis rates were measured. (**B**) The time course was followed by HPLC and the concentrations of substrates and products were calculated from the integrated peak areas of the chromatograms (**A**). It is noteworthy that formation of Man4 (middle panel) and Man5 (bottom panel) results from the transglycosylation reactions. The fastest hydrolysed oligosaccharide is Man6 (bottom panel).

The oligosaccharides with DPs of 4–7 that accumulated were likely to be substituted galactomanno-oligosaccharides, in which the α-D-galactosyl substituent could not be by-passed by the HvβMANNOS1. These oligosaccharides were not hydrolysed, even after prolonged incubation for 18 h at 30 °C with the two enzymes (Figure 3).

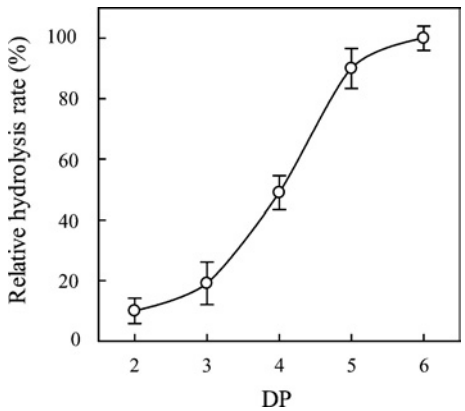

Figure 5 Relative rates of hydrolysis of Man2–Man6 by HvβMANNOS1

Hydrolysis rates are expressed as the percentage of highest rate, which was observed for Man6. Standard errors of triplicate assays are within 4–7 %.

Substrate specificity of HvβMANNOS1

The relative rates of hydrolysis of a series of 4NP glycosides by the purified HvβMANNOS1 are shown in Table 4. The 4NP-Man substrate was preferred by the enzyme, the rate of hydrolysis of 4NP-Glc was slower but significant, and other 4NP β-D-glycosides were hydrolysed slowly, if at all (Table 4). When hydrolytic rates were determined with the (1,4)-β-D-manno-oligosaccharide series Man2 to Man6, the rate increased markedly with the DP of the substrate (Figure 5).

The barley (1,4)-β-D-mannan endohydrolase gene family

The sequences of 35 N-terminal amino acid residues and of five tryptic peptides generated from the purified barley HvMAN1 enzyme were determined (results not shown) and used to design PCR primers. A PCR product was subsequently generated and its sequence shown to include perfect matches of tryptic peptides. However, it proved difficult to isolate a full-length cDNA. When the PCR product was used to screen a cDNA library, no full-length cDNAs were found. Similarly, attempts to use 5′- or 3′-RACE (rapid amplification of cDNA ends) [36] were unsuccessful, and the full-length cDNA sequence was eventually obtained by chromosomal walking from the 5′- and 3′-ends of sequences from the PCR product. The sequence of 379 amino acid residues of the mature enzyme encoded by the gene is shown in Figure 6, together with the positions of the tryptic peptides. The positions of the catalytic amino acid residues were deduced from the conserved regions of other family GH5 glycoside hydrolases [37]; Glu^{179} is the catalytic acid/base and Glu^{298} is the catalytic nucleophile. The molecular mass of the mature enzyme calculated from the amino acid sequence is 42036 Da. The enzyme has one potential N-glycosylation site, but no disulfide bridges (Figure 6). Seven out of nine putative amino acid residues that are predicted to be involved in substrate binding are absolutely conserved in the HvMAN1 and three other plant (1,4)-β-D-mannan endohydrolases (marked by light shaded panels in Figure 6). The nucleotide and amino acid sequences of the barley HvMAN1 mature enzyme were deposited in the GenBank®/EBI Data Bank with accession number DQ356891.

Searches of the barley EST (expressed sequence tag) databases revealed no sequences corresponding directly to the HvMAN1 enzyme purified here, but a total of 53 EST sequences with sequence identities of 70–91 % over matching regions of the *HvMAN1* cDNA sequence were detected. These EST sequences

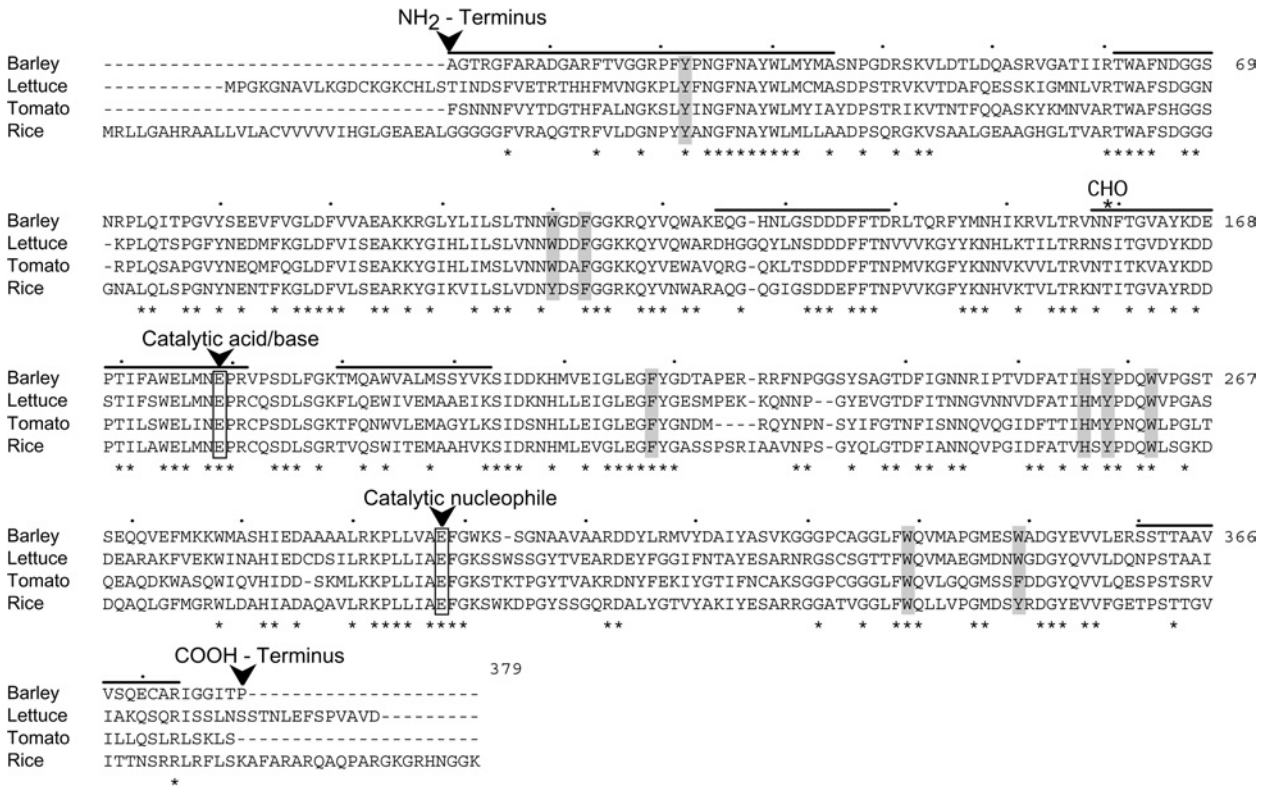

Figure 6 Alignment of plant family GH5 (1,4)-β-D-mannan endohydrolases

The amino acid residues from barley HvMAN1 (the present study), lettuce (Swiss-Prot accession number Q93X40), tomato (Q8L5J1) and rice (Q8LR27) were aligned with T-COFFEE [28]. The residues are numbered for the barley HvMAN1 from the N to C-terminal amino acid residues (arrowheads) and every 10th amino acid residue is indicated by a dot. Potential N-glycosylation site in HvMAN1 is marked by CHO. Two arrowheads within the sequence point at the putative catalytic nucleophile (Glu^{171} for HvMAN1) and putative catalytic acid/base (Glu^{290} for HvMAN1). Identical residues in both sequences are indicated by asterisks. Black over-lines above the sequence of HvMAN1 indicate the N-terminal and internal amino acid sequences that were analysed by Edman degradation, after proteolytic cleavage by trypsin. The light shaded residues are conserved aromatic residues that are believed to be involved in substrate binding.

correspond to five individual genes with unique primary amino acid sequences, and are believed to encode other barley (1,4)-β-D-mannan endohydrolase isoenzymes. Thus, with the gene encoding the (1,4)-β-D-mannan endohydrolase HvMAN1 purified here, it can be concluded that at least six *HvMAN* genes are present in barley.

Molecular modelling of HvMAN1

The tomato (1,4)-β-D-mannan endohydrolase crystal structure 1RH9 was used as a template for molecular modelling of the barley HvMAN1. The positions of sequences of the HvMAN1 and the tomato enzyme on an unrooted radial phylogenetic tree of a plant family GH5 (1,4)-β-D-mannan endohydrolase indicated that the two enzymes were related (Figure 7). A total of 361 amino acid residues from 373 amino acid residues of the tomato enzyme were used for modelling. The sequence identity and similarity scores of 54.7 and 73.6 % respectively between the template tomato structure and target HvMAN1 sequences indicated that there is more than 95 % certainty that the template sequence is optimal for molecular modelling. Pairwise alignment showed one gap after amino acid residue 306 in HvMAN1 and four gaps each after amino acid residues 69, 209, 216 and 279 in the tomato sequence (results not shown).

All amino acid residues of the modelled HvMAN1 structure, calculated by PROCHECK, were located in the most favoured or additionally allowed regions of the Ramachandran plot [33] with overall average G-factor values (measures of normality of main chain bond lengths and bond angles), of 0.18 and 0.12, for the template and HvMAN1 3D structures respectively. The Z-score values were -10.43 and -10.04 for the template and HvMAN1 3D structures respectively, reflecting combined energy profiles. The quality of the model was further evaluated through the pG server [32] and the value pG = 1 for HvMAN1 was calculated. Taken together, these analyses indicated that HvMAN1 model was reliable.

Different views of 3D model of the barley HvMAN1 (Figure 8) show that the structure adopts a $(\beta/\alpha)_8$ TIM barrel fold and has a deep substrate binding cleft, where catalytic and substrate-binding amino acid residues are positioned; these amino acid residues are shown in space-filling representation with van der Waals radii in red and blue colours (Figure 8B). The morphology of the substrate-binding clefts and charge distributions mapped on molecular surfaces of the tomato and the barley (1,4)-β-D-mannan endohydrolases are highly conserved (Figures 8C and 8D). Superposition of the modelled HvMAN1 and the template tomato enzyme 1RH9 3D structures over the Cα backbone positions showed an rmsd value of 1.120 Å for 361 amino acid residues calculated from 366 residues of the model (99 % of all amino acid residues).

Transcript analysis of the *HvMAN1* gene

The Q-PCR analysis of *HvMAN1* transcript abundance in a range of barley tissues, described in [26], showed the mRNA to be most abundant in the maturation zone of young roots, in first leaf

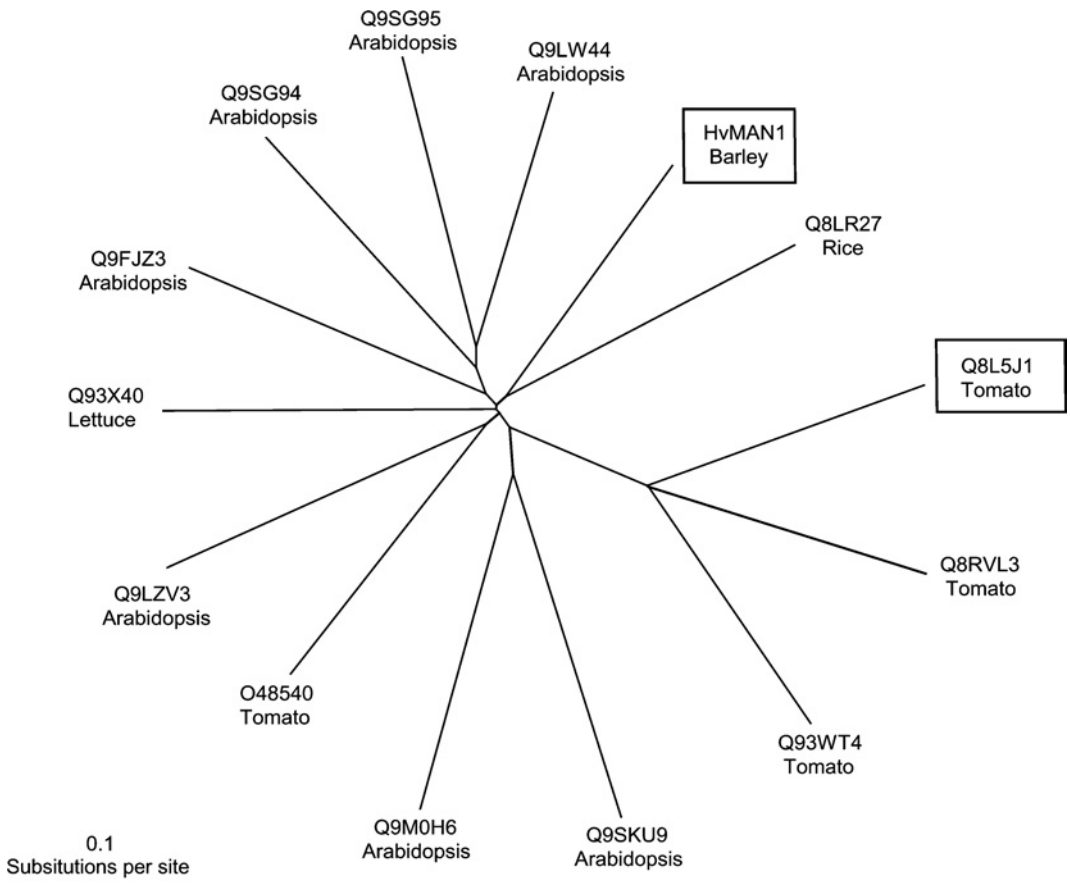

Figure 7 Unrooted radial phylogenetic tree of plant family GH5 (1,4)-β-D-mannan endohydrolases

Amino acid sequences were aligned with T-COFFEE [28]. Branch lengths are drawn to scale. The Swiss-Prot accession numbers of the sequences are shown. The barley HvMAN1 and the tomato enzyme (used as a template for molecular modelling; cf. Figure 8) are placed in a box.

tips and in stems (Figure 9A). Slightly higher levels of *HvMAN1* mRNA are detected in developing grain endosperm after various days of pollination, with peak abundance after 3 days (Figure 9B).

DISCUSSION

The purification procedure described in Scheme 1 yielded a highly purified (1,4)-β-D-mannan endohydrolase, designated HvMAN1, and a single protein band was seen on SDS/PAGE and IEF gels, which gave a single N-terminal amino acid sequence. The enzyme was recovered from barley seedlings 10 days after germination and, although it is difficult to define the precise source of the enzyme at this stage, it is likely to have arisen from tissues in the seedling rather than in the grain itself. Overall, the enzyme proved to be relatively unstable at all stages of the purification procedure. Essentially all activity was lost if the enzyme was frozen and thawed once, unless BSA was added, and activity decreased steadily when the enzyme was stored on ice. Similar difficulties were experienced during purification of a barley (1,4)-β-D-xylan endohydrolase [38], while other hydrolases from barley such as (1,3)- and (1;3,1,4)-β-D-glucan endohydrolase [18,39], β-D-glucan glucohydrolase and β-D-glucosidase [19], arabinoxylan arabinofuranohydrolase [40], or α-L-arabinofuranosidase and β-D-xylosidase [41] were relatively stable. Thus, to maximize the yields of the HvMAN1, the purification procedure was performed at 0–4 °C as quickly as possible, and the enzyme was never frozen during the purification procedure. Furthermore, the addition of 2-mercaptoethanol was necessary to prevent rapid loss of activity. The inherent instability of the enzyme probably explains why the final yield was only 0.3 % of the activity detected in the initial seedling extracts (Table 1).

During purification, unexpectedly high levels of β-D-mannosidase activity, as assayed using 4NP-Man as substrate, were detected (Figure 1; Table 4). When the β-D-mannosidase was purified, it was shown to be the same enzyme that had been purified previously from barley, but which had been designated a β-D-glucosidase isoenzyme βII from the GH1 family of glycoside hydrolases [15,16,37]. Thus a chance that the two enzymes represent two different, yet closely related glycosidases is negligible. A preference of the barley β-D-glucosidase, now designated HvβMANNOS1, for (1,4)-β-D-manno-oligosaccharides had been predicted and verified previously, based on analysis of family GH1 enzymes from *Arabidopsis thaliana* [42]. More specifically, Xu et al. [42] identified structural differences in the genes and diagnostic amino acid sequence motifs in family GH1 members, with preferences for β-D-mannosides or for β-D-glucosides. Thus the L(S/A)ENG active site motif was associated with preferences for β-D-mannosides, while (I/V)TENG motif was linked to β-D-glucosides [42]; the motif of the barley HvMANNOS1 is LSENG [15,16]. Here, the relative rates of hydrolysis of the β-D-mannosides by the barley enzyme

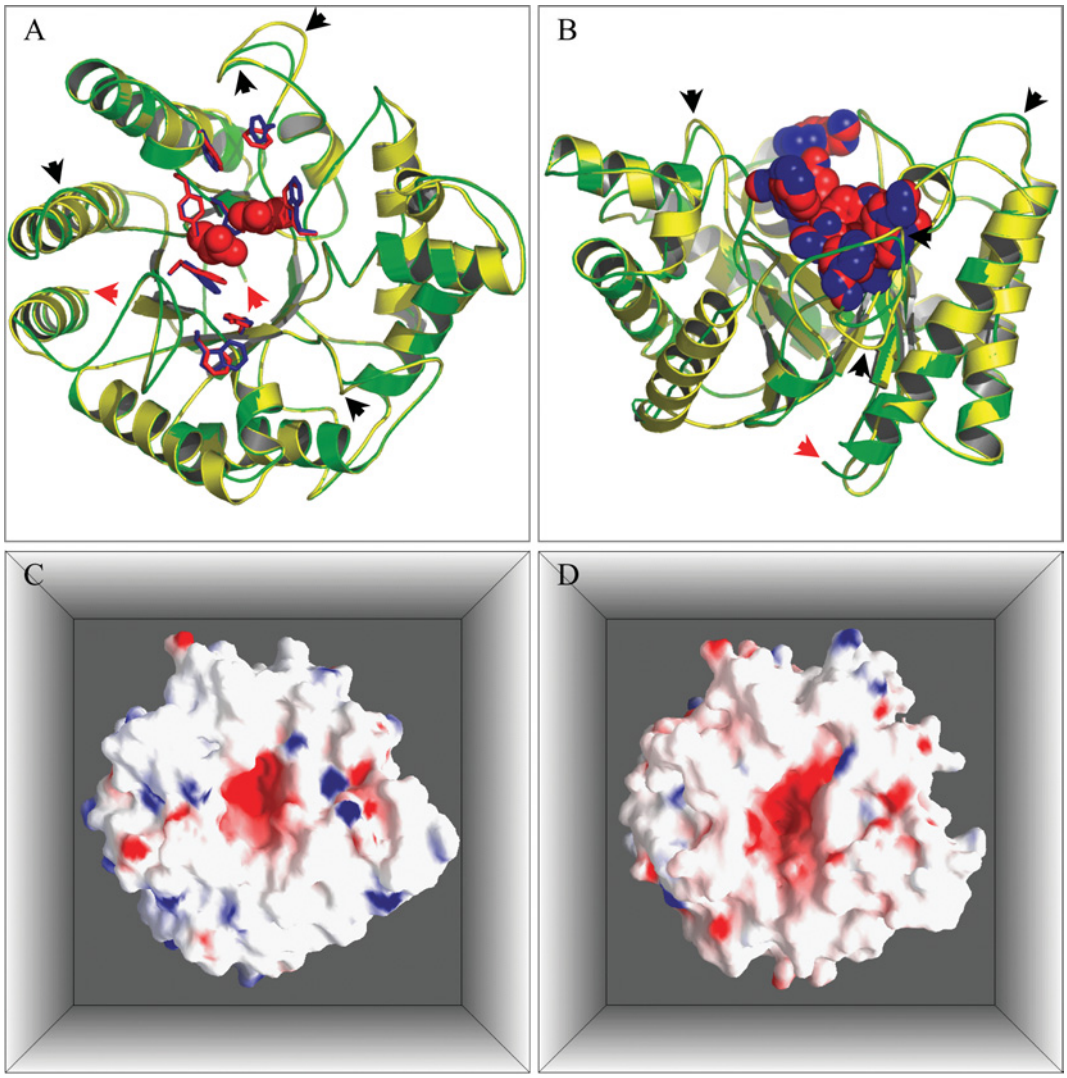

Figure 8 Molecular model of HvMAN1

(**A**) Superposition of the modelled HvMAN1 (yellow) and the template tomato (1,4)-β-D-mannan endohydrolase 1RH9 (green) structures over the Cα backbone positions (rmsd value is 1.120 Å for 361 amino acid residues) showing the $(\alpha/\beta)_8$ TIM barrel fold with secondary structural elements. The central and right-hand-side red arrows indicate N- and C-termini respectively. Black arrows point to the four insertions in HvMAN1, which are located in the loop regions. Red spheres indicate conserved catalytic amino acid residues, and red and blue sticks indicate conserved substrate-binding amino acid residues in the modelled and the template structures (cf. Figure 6). (**B**) The deep cleft represents the substrate-binding cleft and its geometry is conserved in both structures. The conserved catalytic and substrate-binding amino acid residues of the modelled barley HvMAN1 (red spheres) and the tomato 1RH9 (blue spheres) structures are shown in space-filling representations with van der Waals radii. (**C**, **D**) Charge distributions mapped on to molecular surfaces of the template (**C**) and the modelled HvMAN1 (**D**) structures. The two panels show molecular surface morphologies coded by electrostatic potential. Blue and red patches indicate electropositive (+21 kT/e) and electronegative (−20 kT/e) regions respectively.

HvβMANNOS1 were shown to increase with the DP of the substrates (Figure 5). Although the products of hydrolysis were not examined in detail, comparison of these results with those obtained for the same enzyme on a series of cellodextrins suggested that the barley enzyme is acting as an exohydrolase [16]. Examination of oligosaccharide products following hydrolysis of galactomannans with a combination of the purified (1,4)-β-D-mannosidase HvβMANNOS1 and the purified (1,4)-β-D-mannan endohydrolase HvMAN1 indicated that the (1,4)-β-D-mannosidase could not by-pass α-D-galactosyl substituents in the main chain of the polysaccharide or of derived oligosaccharides (Figure 3). The barley HvβMANNOS1 was not examined further in the present study.

However, the enzymic and kinetic properties of the purified (1,4)-β-D-mannan endohydrolase HvMAN1 were defined in detail. The purified enzyme had a pH optimum against LB-GM of 4.75 and the bell-shaped pH versus activity curve indicated that at least two ionizable amino acid residues were required for activity; one was likely to be the catalytic nucleophile with an apparent pK_a of approx. 4.0 and the other was likely to be the catalytic acid/base, with an apparent pK_a of approx. 5.3 (see Supplementary Figure 2). Using LB-GM as the substrate, the K_m and k_{cat} values for the purified HvMAN1 enzyme were 0.16 mg/ml and 12.9 s^{-1} respectively, while the catalytic efficiency (k_{cat}/K_m) was 80.9 $s^{-1} \cdot ml \cdot mg^{-1}$ (Table 2). The purified HvMAN1 enzyme had an apparent molecular mass of 43 kDa based on its mobility during SDS/PAGE (Figure 2), which is close to the value of 42 036 Da predicted from the corresponding cDNA (Figure 6). Whether or not this difference results from glycosylation of the single potential N-glycosylation site detected in the full amino

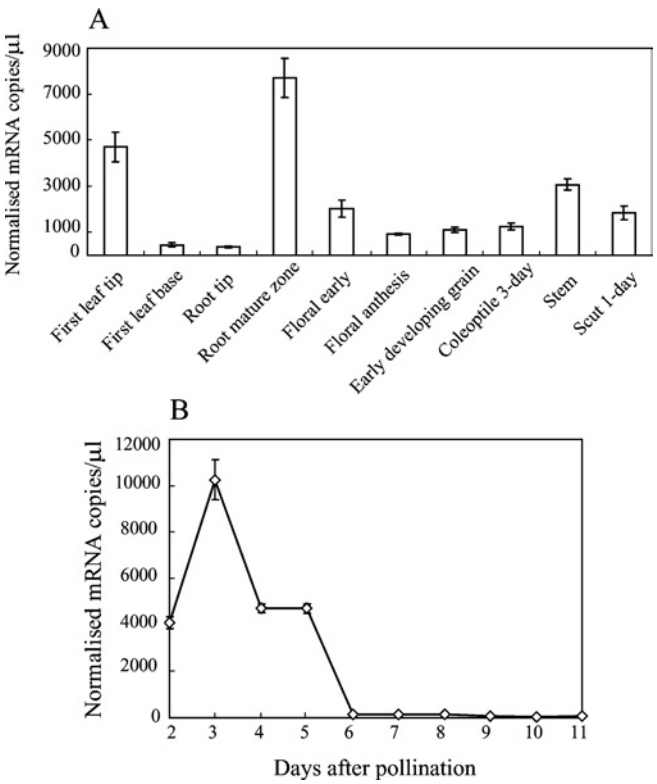

Figure 9 Transcript analyses of *HvMAN1* gene

(**A**) *HvMAN1* gene transcript levels measured in a range of barley tissues described in [26], using Q-PCR. (**B**) *HvMAN1* gene transcript levels measured in extracts of developing barley endosperm at various times after pollination, using Q-PCR.

acid sequence deduced from the cDNA (Figure 6) is not known. The cDNA encoded an enzyme of 379 amino acid residues, and comparisons of its sequence with those of other plant (1,4)-β-D-mannan endohydrolases indicated that the enzymes are not highly conserved (Figure 6). The C-terminal amino acid sequences in (1,4)-β-D-mannan endohydrolases from different tomato cultivars are key determinants of enzyme activity [43], but there is little or no similarity in the C-terminal amino acid sequences of the barley enzyme and other plant (1,4)-β-D-mannan endohydrolases in the databases (Figure 6).

The substrate specificity of the purified (1,4)-β-D-mannan endohydrolase HvMAN1 was examined by screening activity against a range of polymeric substrates and glycosides (Table 3). Activity was largely confined to polymeric, (1,4)-β-linked mannans, glucomannans and galactomannans, and appeared to be enhanced by the presence of α-D-galactosyl substituents. Unsubstituted ivory nut mannan was hydrolysed more slowly, most likely due to its insolubility, than guar or locust-bean galactomannans, while the guar galactomannan, which had an intermediate Man/Gal ratio, was hydrolysed relatively rapidly. Thus it appeared that unsubstituted regions of galactomannans were required for hydrolysis, but that a minimal number of α-D-galactosyl residues might be necessary for maximal hydrolytic rates. The glucomannan substrate was also hydrolysed at a significant rate (Table 3), but it remains to be determined if Man–Glc glycosidic linkages, or only Man–Man, or both, are hydrolysed by HvMAN1. In contrast, the catalytic rate constant k_{cat} of the HvMAN1 on mannopentaitol was approximately three times lower than that calculated for LB-GM (Table 2). Presumably, the reductive modification of the reducing terminal mannosyl residue of Man5, which most likely shortens the Man5 oligosaccharide by a reduced Man residue, was responsible for this decrease in catalytic efficiency.

The products of hydrolysis of LB-GM included manno-oligosaccharides and probably galactomanno-oligosaccharides, but very little Man was released (Figure 3, left panel). This action pattern was typical of polysaccharide endo-hydrolases, and it was therefore concluded that the HvMAN1 enzyme from barley was a (1,4)-β-D-mannan endohydrolase or β-D-mannanase (EC 3.2.1.78).

To investigate the position of the catalytic amino acid residues with respect to the β-D-mannosyl-binding subsites in the HvMAN1 active site, the rates of hydrolysis of and the products released from the manno-oligosaccharide series with DPs 4–6 were examined (Figure 4). Overall, the initial rates of hydrolysis increased with DP. This indicated that the substrate-binding site consisted of at least six binding subsites. Furthermore, oligomeric products indicated that the catalytic amino acid residues were probably located between the central subsites on the enzyme, as follows:

Man-Man-Man $\downarrow$ Man-Man-Man.

The absence of Man among the products of Man4 hydrolysis suggested that when a non-reducing terminal glycosidic linkage was hydrolysed to produce Man3 and Man, the Man was transferred by transglycosylation reactions to Man2, to form Man3. Similarly, during Man5 and Man6 hydrolysis, no Man was released, although the presence of Man4 and Man5 respectively suggested that non-reducing terminal linkages were being hydrolysed with simulaneous mannosyl transfer to the second substrate molecule or to other oligosaccharide acceptors. Taken together, these results indicated that HvMAN1 hydrolysed Man4–Man6 through transglycosylation reactions at low substrate concentrations. Transglycosylation is not uncommon in retaining polysaccharide endo-hydrolases, where reversal of a hydrolytic reaction can occur in the presence of a large excess of substrate. However, HvMAN1 catalyses these reactions at both low and high substrate concentrations, and the yields of transglycosylation products are proportional to initial substrate concentrations (Figure 3, right panel; Figure 4). Therefore transglycosylation could be a part of a hydrolytic mechanism of HvMAN1. These thermodynamically controlled synthetic reactions could be considered as a mechanistic consequence of catalysis itself, and it needs to be determined *in planta* if transglycosylation reactions catalysed by HvMAN1 have a significant biological function. The transglycosylation activity of the barley HvMAN1 enzyme is unlikely to correspond to the type of mannan transglycosylase activity (results not shown) that has been reported in cell walls of kiwifruit species (*Actinidia*) and tomato (*Solanum lycopersicon*) [44].

The 3D structure of the barley HvMAN1 enzyme was modelled upon the experimentally determined 3D structure of the tomato (1,4)-β-D-mannan endohydrolase [14]. Although the two enzymes share only approx. 54 % amino acid sequence identity, reliable models of the barley HvMAN1 were obtained (Figure 8). The rmsd value over 361 residues was 1.120 Å, when the model was superposed upon the template structure. A model is usually considered reliable when the rmsd value is approx. 1 Å for an overall 50 % sequence identity. In common with other family GH5 enzymes [14], the barley HvMAN1 adopts a canonical $(\beta/\alpha)_8$ fold and is globular in shape, but is characterized by the presence of a deep groove that extends over the surface of the molecule (Figure 8). This groove represents the substrate-binding cleft of the enzyme and its geometry is conserved in the tomato and barley

3D structures. The length of the cleft is consistent with a substrate-binding site corresponding to six or seven (1,4)-β-D-mannosyl residues. This in turn is consistent with product analyses that indicate that the enzyme has at least six substrate-binding subsites (Figure 4). The putative catalytic amino acid residues, Glu^{179} and Glu^{298}, are located close to the centre of the cleft. The catalytic nucleophile Glu^{298} and catalytic acid/base Glu^{179} are 5–6 Å apart, at the ends of β-strands 4 and 7 respectively. These arrangements are typical of retaining polysaccharide endohydrolases [14,45].

The substrate-binding cleft that extends across the barley HvMAN1 is predicted to be V-shaped, and the molecular model further predicts that significant distortion of either an unsubstituted (1,4)-β-D-mannan or a (1,4)-β-D-glucomannan would occur during substrate binding. In particular, the glycosyl residue at subsite -1 is likely to adopt a distorted $^{1}S_{3}$ or a similar ^{4}E conformation, in agreement with other results for family GH5 enzymes [14]. The shape of the substrate-binding groove also indicates that the enzyme would have little capacity to bind mannosyl residues substituted with bulky α-D-galactosyl substituents, which is consistent with the observation that 6^{3},6^{4}-di-α-D-galactosyl Man5 is not hydrolysed by the enzyme, while unsubstituted (1,4)-β-D-manno-oligosaccharides of DP 3–6 are hydrolysed at significant rates (Tables 2 and 3; cf. Figure 4). Nevertheless, the substrate specificity analyses suggested that galactomannans with limited α-D-galactosyl substitution were hydrolysed more rapidly than unsubstituted (1,4)-β-D-mannans (Table 3). It is not yet possible to explain this apparent anomaly in precise structural terms. It would also be predicted from the available 3D structures and models that family GH5 (1,4)-β-D-mannan endohydrolases would have a wider cleft than family GH5 cellulases, because the C2-OH groups of the (1,4)-β-D-mannan substrates are axial, while those of the (1,4)-β-D-glucan substrates of cellulases are equatorial in configuration [14,46].

The structural model of the barley HvMAN1 offers a possible explanation for the instability of the enzyme observed during its purification. Although the barley enzyme has cysteine residues at positions 325 and 363, Cys^{325} is buried within the enzyme and cannot form a disulfide bond with Cys^{363}. Thus there are no disulfide bridges in the barley HvMAN1 3D model. Similarly, there are no disulfide bridges in the tomato (1,4)-β-D-mannan endohydrolase [14]. The absence of disulfide bridges might be responsible for the relative instability of the barley HvMAN1, and it might be predicted that the tomato enzyme would also be unstable. In contrast, bacterial and fungal family GH5 (1,4)-β-D-mannan endohydrolases usually have several disulfide bridges. For example, the (1,4)-β-D-mannan endohydrolase from *Trichoderma* has four disulfide bridges [46].

When the partly purified barley HvMAN1 was subjected to IEF, a major band of pI 7.8 was detected, but a fainter band of pI 7.4 was also seen (results not shown). This suggested that more than one (1,4)-β-D-mannan endohydrolase might be present in barley. Subsequent searches of the barley EST databases, which currently include close to 410000 entries, failed to identify any sequences that corresponded exactly to the HvMAN1 sequence. However, it was clear that the databases contained sequences for five other (1,4)-β-D-mannan endohydrolases, and it was therefore concluded that the barley genome contains at least six *HvMAN* genes. This may be compared with the rice and *Arabidopsis* genomes, which contain nine and ten putative (1,4)-β-D-mannan endohydrolase genes respectively.

It was also apparent that the barley *HvMAN1* gene must be expressed at relatively low levels, at least in the tissues extracts used for the generation of the EST libraries. This was confirmed here through quantitative transcript analyses using Q-PCR, where the abundance of mRNA encoding the *HvMAN1* gene was relatively low in all tissue extracts examined (Figure 9A) [26]. Wang et al. [47] detected both (1,4)-β-D-mannan endohydrolase and β-D-mannosidase activities in germinated rice grain, and concluded that the endohydrolase was predominantly synthesized in the aleurone layer. Some (1,4)-β-D-mannan endohydrolase mRNA was detected in the scutellum of germinated barley grain in the present study (Figure 9A), although levels in the aleurone layer of germinated barley were not measured. The highest levels of *HvMAN1* transcripts were detected in early developing endosperm of barley, where levels increased to a maximum 3 days after pollination and thereafter declined to undetectable levels 6 days after pollination (Figure 9B). It is noteworthy that Man-containing polysaccharides have been detected in the cell walls of developing barley endosperm 6 days after pollination [48], but that the final levels of Man-containing polysaccharides in the walls are only approx. 2 % by weight [7]. Whether or not low levels of (1,4)-β-D-mannan endohydrolases are required for mannan or glucomannan synthesis, or for turnover of these polysaccharides, is not known at present, although there is mounting evidence that cellulases are often present in plant cells during cellulose synthesis and that the cellulases are indeed essential for correct cellulose assembly in the wall. A point mutation in the *Ar. thaliana* KORRIGAN gene (*KOR*), which encodes a cellulase, causes a large reduction in wall cellulose [49]. How the cellulase is involved in cellulose synthesis is unknown, but it might involve trimming or 'editing' nascent cellulose chains [49], or possibly releasing newly synthesized chains from the biosynthetic enzymes. The availability of cDNAs encoding barley (1,4)-β-D-mannan endohydrolases, together with the recent identification of the cellulose synthase-like *CslA* gene family as mannan synthases [50], now enables the possible role of the hydrolytic enzymes in wall biosynthesis to be tested.

We thank Neil Shirley (School of Agriculture, Food and Wine, University of Adelaide and Australian Centre for Plant Functional Genomics) for assistance with the Q-PCR transcript analyses. Francois Taravel from Centre de Recherches sur les Macromolécules Végétales (Grenoble, France) is acknowledged for providing a collection of native and modified galactomannans. Aaron J. Oakley from the Research School of Chemistry at the Australian National University is thanked for providing (before release) the co-ordinates of the structure of a tomato (1,4)-β-D-mannan endohydrolase. This work was supported by grants from the Australian Research Council (to G. B. F. and M. H.) and the Grains Research and Development Corporation (to G. B. F.).

REFERENCES

1 Harris, P. J. (2005) Non-cellulosic polysaccharides in plant cell walls. In The Hemicelluloses Workshop 2005 (Entwistle, K. M. and Walker, J. C. F., eds.), pp. 13–35, University of Canterbury, Christchurch, New Zealand
2 Dea, I. C. M. and Morrison, A. (1975) Chemistry and interactions of seed galactomannans. Adv. Carbohydr. Chem. Biochem. **31**, 241–312
3 Reid, J. S. G. and Edwards, M. (1995) Galactomannans and other cell wall storage polysaccharides. In Food Polysaccharides and Their Applications (Stephen, A. M., ed.), pp. 155–186, Marcel Dekker, New York
4 Avigad, G. and Dey, P. M. (1997) Carbohydrate metabolism: storage carbohydrates. In Plant Biochemistry (Dey, P. M. and Harborne, J. B., eds.), pp. 143–204, Academic Press, San Diego and London
5 Katsuraya, K., Okuyama, K., Hatanaka, H., Oshima, R., Sato, T. and Matsuzaki, K. (2003) Constitution of konjac glucomannan: chemical analysis and ^{13}C NMR spectroscopy. Carbohydr. Polym. **53**, 183–189
6 Gibeaut, D. M., Pauly, M., Bacic, A. and Fincher, G. B. (2005) Changes in cell wall polysaccharides in developing barley (*Hordeum vulgare*) coleoptiles. Planta **390**, 105–113
7 Fincher, G. (1975) Morphology and chemical composition of barley endosperm cell walls. J. Inst. Brew. (London) **81**, 116–122
8 Bacic, A., Harris, P. J. and Stone, B. A. (1988) Structure and function of plant cell walls. In The Biochemistry of Plants (Priess, J., ed.), pp. 297–371, Academic Press, New York
9 Shibuya, N. and Misaki, A. (1978) Structure of hemicellulose isolated from rice endosperm cell wall: mode of linkage and sequences in xyloglucan, β-D-glucan and arabinoxylan. Agric. Biol. Chem. **42**, 2267–2274

10 Nonogaki, H., Nomaguchi, M. and Morohashi, Y. (1995) Endo-β-mannanases in the endosperm of germinated tomato seeds. Physiol. Plant **94**, 328–334
11 Bewley, J. D., Burton, R. A., Morohashi, Y. and Fincher, G. B. (1997) Molecular cloning of a cDNA encoding a (1 → 4)-β-mannan endohydrolase from the seeds of germinated *tomato* (*Lycopersicon esculentum*). Planta **203**, 454–459
12 Still, D. W. and Bradford, K. J. (1997) Endo-β-mannanase activity from individual tomato endosperm tissues in relation to germination. Plant Physiol. **113**, 21–29
13 Mo, B. and Bewley, J. D. (2002) β-Mannosidase (EC 3.2.1.25) activity during and following germination of tomato (*Lycopersicon esculentum* Mill.) seeds. Purification, cloning and characterization. Planta **215**, 141–152
14 Bourgault, R., Oakley, A. J., Bewley, J. D. and Wilce, M. C. (2005) Three-dimensional structure of (1,4)-β-D-mannan mannanohydrolase from tomato fruit. Protein Sci. **14**, 1233–1241
15 Leah, R., Kigel, J., Svendsen, I. and Mundy, J. (1995) Biochemical and molecular characterization of a barley seed β-glucosidase. J. Biol. Chem. **270**, 15789–15797
16 Hrmova, M., MacGregor, E. A., Biely, P., Stewart, R. J. and Fincher, G. B. (1998) Substrate binding and catalytic mechanism of a barley β-D-glucosidase/(1,4)-β-D-glucan exohydrolase. J. Biol. Chem. **273**, 11134–11143
17 Kremnicky, L., Slavikova, E., Mislovicova, D. and Biely, P. (1996) Production of extracellular β-mannanases by yeasts and yeast-like microorganisms. Folia Microbiol. **41**, 43–47
18 Hrmova, M. and Fincher, G. B. (1993) Purification and properties of three (1 → 3)-β-D-glucanase isoenzymes from young leaves of barley (*Hordeum vulgare*). Biochem. J. **289**, 453–461
19 Hrmova, M., Harvey, A. J., Wang, J., Shirley, N. J., Jones, G. P., Stone, B. A., Høj, P. B. and Fincher, G. B. (1996) Barley β-D-glucan exohydrolases with β-D-glucosidase activity. Purification and determination of primary structure from a cDNA clone. J. Biol. Chem. **271**, 5277–5286
20 Harvey, A. J., Hrmova, M. and Fincher, G. B. (2001) Regulation of genes encoding β-D-glucan endohydrolases in barley (*Hordeum vulgare* L.). Physiol. Plant **113**, 108–120
21 Somogyi, M. (1952) Notes on sugar determination. J. Biol. Chem. **195**, 19–23
22 Nelson, N. (1944) A photometric adaptation of the Somogyi method for the determination of glucose. J. Biol. Chem. **153**, 375–380
23 Wolfrom, M. L. and Anno, K. (1952) Transition metal catalyzed selective oxidation of sugars and polyols. J. Am. Chem. Soc. **74**, 5583–5584
24 Marquart, D. W. (1963) An algorithm for the least-squares estimation of nonlinear parameters. J. Soc. Ind. Appl. Math. **11**, 431–441
25 Leatherbarrow, R. J. (1998) Grafit Users's Guide, Grafit version 4.0, p. 234, Erithacus Software Ltd., Horley, Surrey
26 Burton, R. A., Shirley, N. J., King, B. J., Harvey, A. J. and Fincher, G. B. (2004) The *CesA* gene family of barley. Quantitative analysis of transcripts reveals two groups of co-expressed genes. Plant Physiol. **134**, 224–236
27 Dellaporta, S. L., Wood, J. and Hicks, J. B. (1983) A plant DNA minipreparation: version II. Plant Mol. Biol. Rep. **1**, 19–21
28 Notredame, C., Higgins, D. and Heringa, J. (2000) T-Coffee: a novel method for fast and accurate multiple sequence alignment. J. Mol. Biol. **302**, 205–217
29 Zhang, Q., Hrmova, M., Shirley, N. J., Lahnstein, J. and Fincher, G. B. (2006) Gene expression patterns and catalytic properties of UDP-glucose 4-epimerases from barley (*Hordeum vulgare* L.). Biochem. J. **394**, 115–124
30 Altschul, S. F., Madden, T. L., Schäffer, A. A., Zhang, J., Zhang, Z., Miller, W. and Lipman, D. J. (1997) Gapped BLAST and PSI-BLAST: a new generation of protein database search programs. Nucleic Acids Res. **25**, 3389–3402
31 Callebaut, I., Labesse, G., Durand, P., Poupon, A., Canard, L., Chomilier, J., Henrissat, B. and Mornon, J. P. (1997) Deciphering protein sequence information through hydrophobic cluster analysis (HCA): current status and perspectives. Cell. Mol. Life Sci. **53**, 621–645
32 Sali, A. and Blundell, T. L. (1993) Comparative protein modelling by satisfaction of spatial restraints. J. Mol. Biol. **234**, 779–815
33 Laskowski, R. A., MacArthur, M. W., Moss, D. S. and Thornton, J. M. (1993) PROCHECK: a program to check the stereochemical quality of protein structures. J. Appl. Cryst. **26**, 283–291
34 Jones, T. A., Zou, J. Y., Cowan, S. W. and Kjeldgaard, M. (1991) Improved methods for building protein models in electron density maps and the location of errors in these models. Acta Crystollogr. Sect. A Found. Crystallogr. **47**, 110–119
35 Nicolls, A., Sharp, K. and Hönig, B. (1991) Protein folding and association: insights from the interfacial and thermodynamic properties of hydrocarbons. Proteins **4**, 281–296
36 Frohman, M. A., Dush, M. K. and Martin, G. R. (1988) Rapid production of full-length cDNAs from rare transcripts: amplification using a single gene-specific oligonucleotide primer. Proc. Natl. Acad. Sci. U.S.A. **85**, 8998–9002
37 Coutinho, P. and Henrissat, B. (1999) Carbohydrate-active enzymes: an integrated database approach. In Recent Advances in Carbohydrate Bioengineering (Gilbert, H., Davies, G., Henrissat, B. and Svensson, B., eds.), pp. 3–12, The Royal Society of Chemistry, Cambridge
38 Slade, A. M., Høj, P. B., Morrice, N. A. and Fincher, G. B. (1989) Purification and characterization of three (1 → 4)-β-D-xylan endohydrolases from germinated barley. Eur. J. Biochem. **185**, 533–539
39 Woodward, J. R. and Fincher, G. B. (1982) Purification and chemical properties of two 1,3;1,4-β-D-glucan endohydrolases from germinating barley. Eur. J. Biochem. **121**, 663–669
40 Lee, R. C., Burton, R. A., Hrmova, M. and Fincher, G. B. (2001) Barley arabinoxylan arabinofuranohydrolases: purification, characterization and determination of primary structures from cDNA clones. Biochem. J. **356**, 181–189
41 Lee, R. C., Hrmova, M., Burton, R. A., Lahnstein, J. and Fincher, G. B. (2003) Bifunctional family 3 glycoside hydrolases from barley with α-L-arabinofuranosidase and β-D-xylosidase activity: characterization, primary structures and COOH-terminal processing. J. Biol. Chem. **278**, 5377–5387
42 Xu, Z., Escamilla-Trevino, L., Zeng, L., Lalgondar, M., Bevan, D., Winkel, B., Mohamed, A., Cheng, C. L., Shih, M. C., Poulton, J. and Esen, A. (2004) Functional genomic analysis of *Arabidopsis thaliana* glycoside hydrolase family 1. Plant Mol. Biol. **55**, 343–367
43 Bourgault, R. and Bewley, J. D. (2002) Variations in its C-terminal amino acids determines whether endo-β-mannanase is active or inactive in ripening fruits of different cultivars. Plant Physiol. **130**, 1254–1262
44 Schröder, R., Wegrzyn, T. F., Bolitho, K. M. and Redgwell, R. J. (2004) Mannan transglycosylase: a novel enzyme activity in cell walls of higher plants. Planta **219**, 590–600
45 Jenkins, J., Lo Leggio, L., Harris, G. and Pickersgill, R. (1995) β-Glucosidase, β-galactosidase, family A cellulases, family F xylanases and two barley glycanases form a superfamily of enzymes with 8-fold β/α architecture and with two conserved glutamates near the carboxy-terminal ends of β-strands four and seven. FEBS Lett. **362**, 281–285
46 Sabini, E., Schubert, H., Murshudov, G., Wilson, K. S., Siika-Aho, M. and Penttilä, M. (2000) The three-dimensional structure of a *Trichoderma reesei* β-mannanase from glycoside hydrolase family 5. Acta Crystollogr. Sect. D Biol. Crystallogr. **56**, 3–13
47 Wang, A., Wang, X., Ren, Y., Gong, X. and Bewley, J. D. (2005) Endo-β-mannanase and β-mannosidase activities in rice grains during and following germination, and the influence of gibberellin and abscisic acid. Seed Sci. Res. **15**, 219–227
48 Wilson, S. M., Burton, R. A., Doblin, M. S., Stone, B. A., Newbigin, E. J., Fincher, G. B. and Bacic, A. (2006) Temporal and spatial appearance of wall polysaccharides during cellularization of barley (*Hordeum vulgare*) endosperm. Planta **224**, 655–667
49 Szyjanowicz, P. M., McKinnon, I., Taylor, N. G., Gardiner, J., Jarvis, M. C. and Turner, S. R. (2004) The *irregular xylem 2* mutant is an allele of *korrigan* that affects the secondary cell wall of *Arabidopsis thaliana*. Plant J. **37**, 730–740
50 Dhugga, K., Barreiro, R., Whitten, B., Stecca, K., Hazebroek, J., Randhawa, G., Dolan, M., Kinney, A., Tomes, D., Nichols, S. and Anderson, P. (2004) Guar seed β-mannan synthase is a member of the cellulose synthase super gene family. Science **303**, 363–366

Received 30 January 2006/26 May 2006; accepted 13 June 2006
Published as BJ Immediate Publication 13 June 2006, doi:10.1042/BJ20060170